A&A 592, A81 (2016)
DOI: 10.1051/0004-6361/201628324

Astronomy & Astrophysics

Interstellar ice analogs: H_2O ice mixtures with CH_3OH and NH_3 in the far-IR region

B. M. Giuliano[1,4], R. Martín-Doménech[1], R. M. Escribano[2], J. Manzano-Santamaría[1,3], and G. M. Muñoz Caro[1]

[1] Centro de Astrobiología, INTA-CSIC, Carretera de Ajalvir, km 4, Torrejón de Ardoz, 28850 Madrid, Spain
e-mail: rmartin@cab.inta-csic.es
[2] Instituto de Estructura de la Materia-Consejo Superior de Investigaciones Científicas (IEM-CSIC), 28006 Madrid, Spain
[3] Dept. de Matemática Aplicada, Ciencia e Ingeniería de Materiales, ESCET, Universidad Rey Juan Carlos. C/ Tulipán s/n, Móstoles 28933 Madrid, Spain
[4] Max-Planck-Institut für extraterrestrische Physik, Giessenbachstrasse 1, 85748 Garching, Germany

Received 17 February 2016 / Accepted 29 May 2016

ABSTRACT

Context. New spectroscopic observations in the far-infrared (IR) range are expected from future planned missions. Although water ice is the only species detected so far in interstellar ices in this range, the presence of ice mixtures requires laboratory characterization of the corresponding spectra.
Aims. We present an investigation on far-IR spectra of binary ice mixtures relevant in various astrophysical environments. The foremost goal is to compare the spectroscopic features of the ice mixtures to those of pure ices, and to search for changes in peak frequencies, intensities, and band strengths of the main bands.
Methods. Mixtures H_2O:CH_3OH and H_2O:NH_3 of different ratios have been deposited on a diamond substrate at astrophysically relevant conditions. We measured the spectra in the near- and mid-IR regions to derive ice column densities that were subsequently used to calculate the apparent band strengths in the far-IR region. We also designed theoretical models to study these mixtures and to predict their spectra.
Results. We recorded spectra of amorphous phases for H_2O:CH_3OH mixtures of different compositions, that is 1:1, 3:1, and 10:1 at 8 K, and compared these mixtures to those obtained after warming. This process involves the appearance of new spectral features and changes in band shapes and band strengths. We also compared the spectra to those of the pure species and to theoretical predictions. We measured apparent band strengths for all the observed features. For H_2O:NH_3 mixtures, the ratios selected were 3:1, 1:1, and 1:3. In this case the spectral variations are even more marked than for the water:methanol samples.
Conclusions. Band strengths in the far-IR are missing in astrophysics literature for ice mixtures. The results presented here are valuable for detecting the presence and composition of such mixtures from future space observations in this spectral region.

Key words. astrochemistry – methods: laboratory: molecular – ISM: molecules – techniques: spectroscopic – infrared: ISM

1. Introduction

Since its first identification in 1979 by Léger et al., water ice has been observed in the interstellar medium (ISM) along several lines of sight and in different sources, mainly in dense molecular clouds. Water is the most abundant component of ice observed in space, however, other molecular species have been identified as minor ice components by their spectroscopic features in the infrared (IR) region. In particular, carbon monoxide is the second most abundant species detected in interstellar ices, followed by carbon dioxide, with abundances up to ~40% relative to water. Other species like methanol, ammonia, and methane are present in the ice mantles with abundances up to ~10% relative to water (see Boogert et al. 2015, and references therein).

The identification of the molecular composition of ices in space relies on preliminary laboratory characterization. Infrared spectroscopy is the main tool used to investigate properties of ices, by collecting information about the vibrational modes of the molecules. From the analysis of band positions and profiles it is possible not only to identify the ice components, but also to determine the ice structure (see, for example, Gerakines et al. 2015, for a critical case regarding pure CH_4 ices) and ultimately, to comprehend the degree of processing of an astronomical ice sample, in terms of thermal history and radiative transfer. An extensive characterization of the spectroscopic properties of ices in the laboratory has been conducted in the past 30 yr. The majority of these data were collected in the near- and mid-IR regions, typically from 1 μm to 25 μm.

In the far-IR region, extending from 25 μm to 500 μm, fewer previous studies have been reported. In particular, Bertie & Whalley (1967), Warren (1984), Moore & Hudson (1992), Smith et al. (1994), Maldoni et al. (1999), and Moore et al. (2001) focused mainly on the determination of optical constants and the analysis of the spectral differences between the amorphous and crystalline structures of water ices. Brown & King (1970) and Warren (1986) analyzed pure carbon dioxide ices, Ferraro et al. (1980), Sill et al. (1980), and Martonchik et al. (1984) investigated pure ammonia ices, and Anderson et al. (1988) reported spectroscopic data for methanol pure ices.

Far-IR studies of water and other astrophysically relevant species have also been reported by Hudgins et al. (1993), Trotta (1996), Schmitt et al. (1998), and Coustenis et al. (1999). Johnson & Atreya (1996) investigated water and carbon dioxide planetary ices. In addition, far-IR spectra of mixed ices of astrophysically relevant species have been investigated by Moore & Hudson (1994).

The intermolecular vibrational modes, which are associated with the far-IR spectroscopic region, can be used to interpret the structure of the condensed phase and to discriminate between structures with different degrees of order. However, band strengths are still needed for quantification purposes. In Giuliano et al. (2014) the infrared band strengths in the 25−500 μm region were measured for pure ices of the most astrophysically relevant species, namely H_2O, CO_2, CH_3OH, and NH_3, at a temperature of 8 K followed by warm up. Despite their presence in interstellar ices, CO and CH_4 do not present any feature in the far-IR region above 100 cm^{-1} and were not included in the study. From these data, the band strengths of the ice samples, both apparent (derived from the IR spectra) and absolute (derived from the optical constants) as defined in the molecular spectroscopy literature (see, e.g., Maeda & Schatz 1961; Wexler 1967; Scrocco et al. 1972) were determined.

In the present work, we extended the same analysis to binary ice mixtures of water with methanol and ammonia in different proportions. We did not study binary mixtures with carbon dioxide since the CO_2 far-IR features fall in a frequency region where the noise level is too high (see Giuliano et al. 2014). The presence of another component in a pure ice is known to affect the position and shape of the vibrational bands and, to some extent, can alter their band strengths. Previous examples of this behavior, estimated in the mid-IR region, can be found in d'Hendecourt & Allamandola (1986), Öberg et al. (2007), and Bouwman et al. (2007). A dramatic example of the change in the band strength values for water and methane ice mixtures is shown in Bossa et al. (2015). In our analysis, the apparent band strengths of the far-IR bands were calculated from the column densities of the different components in the ice mixtures.

2. Methods

Characterization of the ice mixtures was performed in the ultra high vacuum (UHV) InterStellar Astrochemistry Chamber (ISAC; described in Muñoz Caro et al. 2010), which is equipped with two external IR-transparent diamond windows that allowed us to collect the whole spectrum of the ice samples during the same experiment. Ice samples were prepared in situ by gas condensation onto a diamond substrate cooled at 8 K by means of a closed-cycle helium cryostat. The diamond substrate presents a small absorption in the 2000−2500 cm^{-1} region, which is compensated by subtracting the window spectrum recorded before the ice deposition.

For preparation of the ice samples, H_2O (triply distilled), CH_3OH (supplied by Panreac, HPLC-gradient grade), and NH_3 (supplied by Praxair, 99.999% pure) were used without further purification. Deposition pressure in our experiments varied between 1×10^{-7}–1×10^{-6} mbar, leading to an approximate deposition rate of between 100−300 ML/min, where 1 ML is 10^{15} molecules cm^{-2}.

The IR spectrum in the 6000−100 cm^{-1} spectroscopic region was recorded at 8 K by Fourier transform infrared (FTIR) transmittance spectroscopy using a Vertex 70 spectrometer equipped with a deuterated triglycine sulfate detector (DTGS). All the spectra were recorded in the near- and mid-IR regions with a resolution of 2 cm^{-1}, aperture 6 mm, and averaged over 128 scan accumulations, while, spectra in the far-IR region were recorded with a resolution of 4 cm^{-1} and 256−512 accumulations. The baseline was corrected manually using a spline function. The ice samples were subsequently heated at a rate of 2−5 K per minute using a silicon diode temperature sensor and a LakeShore Model 331 temperature controller. Warming up of the ice analogs was carried out until a more ordered structure was achieved, evidenced by changes in their IR spectra. Characterization of the ice mixtures was thus performed at both the amorphous state at 8 K and at more ordered structure at higher temperatures.

The column density of the deposited ice was calculated using the formula

$$N = \frac{1}{A}\int_{\text{band}} \tau_\nu \mathrm{d}\nu \tag{1}$$

for bands in the near- and mid-IR region of the spectrum, where N is the column density in cm^{-2}, τ_ν the optical depth of the band, dν the wavenumber differential in cm^{-1}, and A the apparent band strength in cm molecule^{-1}.

For the H_2O:NH_3 ice samples, the adopted band strengths for pure ammonia and water ices are taken from Sandford & Allamandola (1993) and Gerakines et al. (1995, 2005; see Table 1). Using these values for ice mixtures introduces an uncertainty of about 20−30% (d'Hendecourt & Allamandola 1986).

In the case of the H_2O:CH_3OH ice mixtures, the mid-IR bands with known band strengths were either saturated owing to the thickness of our ice samples or blended with features from the other species. Column densities were derived alternatively from the peak height of the 2827 cm^{-1} and the 1660 cm^{-1} bands of methanol and water, respectively. Both peaks corresponded to nonsaturated bands and blending was negligible at the peak position. The relations between the peak heights and column densities of both components were derived using thinner binary ice mixtures whose column densities could be calculated using the above formula. Derived relations are written as

$$N_{H_2O} = (29\,067 \times \tau_{1660\ \mathrm{cm^{-1}}} - 300) \times 10^{15}\ \text{molecules cm}^{-2} \tag{2}$$

$$N_{CH_3OH} = (3804 \times \tau_{2827\ \mathrm{cm^{-1}}} + 4) \times 10^{15}\ \text{molecules cm}^{-2}. \tag{3}$$

Equation (2) is only valid for thick ices ($N_{H_2O} \geq$ 500 molecules cm^{-2}).

Observed bands in the far-IR region were assigned to one of the components in the ice mixture by comparison with the pure ice spectra. Knowing the column density of each component in the ice mixtures allowed us to quantify the apparent band strengths of the corresponding far-IR features in the mixtures, at both low and high temperatures, using the equation

$$A_{\text{FIR}} = \frac{1}{N}\int_{\text{band}} \tau_\nu \mathrm{d}\nu = \frac{\int_{\text{band}}^{\text{FIR}} \tau_\nu \mathrm{d}\nu}{\int_{\text{band}}^{\text{MIR/NIR}} \tau_\nu \mathrm{d}\nu} A_{\text{MIR/NIR}}, \tag{4}$$

which follows from Eq. (1). Calculated A_{FIR} values are affected by the 20−30% uncertainty assumed for the $A_{\text{MIR/NIR}}$ values in the mixtures for using band strengths of the pure ices. In addition, we estimated an uncertainty of ~25% in the determination of the integrated optical depths for the far-IR features. This uncertainty comes from the difficulty in establishing a proper baseline for the IR bands, especially those of water, because of the elevated noise in the low-frequency region of the spectrum. Adding up the uncertainty in the ice column densities mentioned above, the total estimated uncertainty in the A_{FIR} values is of about 50%.

A Pfeiffer Prisma Quadrupole Mass Spectometer (QMS) was used during the experiments to monitor any ice losses that could take place owing to thermal desorption during the warm up of the ice samples. The QMS was equipped with a Channeltron detector of mass spectral range from 1 to 200 amu. Gas-phase molecules were ionized via low-energy (~70 eV) electron bombardment. A rise in the ion current of the mass fragments

Table 1. Band strength (A) values of measured bands in the mid-IR region used for determination of the A values in the far-IR.

Species	Frequency (cm^{-1})	Mode	A (cm $molec^{-1}$)	Reference
NH_3	4995	$\nu_1+\nu_4$ (?)	8.1×10^{-19}	a
	4482	$\nu_1+\nu_2$ (?)	8.7×10^{-19}	a
	1070	ν_2	1.7×10^{-17}	b
H_2O	760	libration	3.1×10^{-17}	c

References. (a) From Gerakines et al. (2005). (b) From Sandford & Allamandola (1993). (c) From Gerakines et al. (1995).

m/z = 18, m/z = 31, and m/z = 15 would be due to desorption of water, methanol, and ammonia molecules, respectively. The high sensitivity of this mass spectrometer allows detection of small quantities of molecules, and it was therefore used preferentially to detect ice losses that may not be detected by the FTIR spectrometer.

We performed several theoretical calculations of mixtures of water and methanol, and water and ammonia molecules, in proportions similar to those in the ice samples recorded in the laboratory experiments. All calculations were carried out using software programs of the Material Studio package from Dassault Systèmes Biovia Corp. We obtained initial geometries with Amorphous Cell, a program that creates cell structures in which molecules are introduced and their interaction energy is minimized by Monte Carlo methods for a given density and temperature. The amorphous modules thus obtained were relaxed with CASTEP (Clark et al. 2005), which employs the density functional theory (DFT) plane-wave pseudo-potential method, for a specified level of accuracy. For our calculations, we chose the generalized gradient approximation with Perdew-Burke-Ernzerhof functionals (Perdew et al. 1996) with convergence thresholds of 5×10^{-6} eV/atom, 0.01 eV/Å, 0.02 GPa and 5×10^{-4} Å for energy, maximum atomic force, maximum cell stress, and maximum atom displacement, respectively; we chose an SCF tolerance of 5×10^{-7} eV/atom.

We predicted spectra at the minimum of the potential energy surface for each structure. We reproduced some spectra in Figs. 1, 4, 6, 9, and 11; in these figures vibrational modes are represented by Lorentzian functions of half width at half maximum (HWHM) of 25 cm^{-1}, which matches the observed features for these amorphous samples. Vibrational mode assignment is provided by the visual tools in Materials Studio, but the modes in this far-IR region are usually blends of atomic motions that include translations and librations, and it is often difficult to point out a single mode. Besides that, the assignments are sometimes too dependent on the final structure, and a small modification in the geometry may enhance one mode over another. Altogether, the assignments proposed here must be taken with caution.

3. Experimental results

As mentioned in previous sections, binary ice mixtures composed of water, which is the major component found in interstellar ices, and methanol or ammonia were characterized in the far-IR region of the spectrum.

Ice samples were deposited at low temperature (8 K) as amorphous solids and subsequently heated. Thermal processing of ices induces structural changes, which may include diffusion of molecules, segregation, and phase transitions to more ordered structures. Characterization of the ice samples was performed at both low and high temperatures, since these structural changes

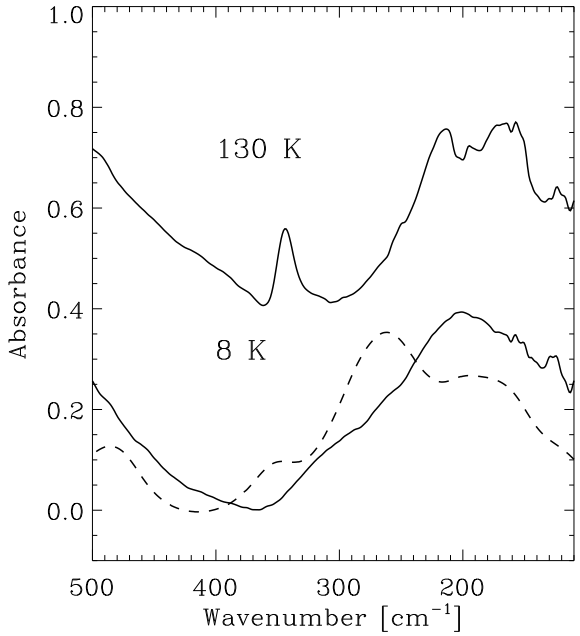

Fig. 1. Infrared spectra of an H_2O:CH_3OH 1:1 ice mixture in the far-IR region at 8 K and 130 K (solid lines). Spectra are offset for clarity. The dashed line represents the calculated spectrum of an ice mixture of the same composition.

produced modifications in the infrared spectra of the ice mixtures, such as the appearance of new features, and/or variations in both the peak frequency and band intensity of those already observed at low temperature.

Peak frequencies were measured and apparent band strengths were derived for every observed feature of both the amorphous mixtures, and the more ordered ices achieved by annealing of the ice samples. These values were compared to the frequencies and band strengths of similar vibrational modes of the amorphous or crystalline pure ices.

Thermal desorption of ice molecules at high temperatures was monitored by means of a QMS. No desorption of water or methanol was detected for the temperatures at which the reported IR spectra were collected, however, desorption of ammonia in the H_2O:NH_3 ice mixtures started above 90 K, before structural changes were complete. This made the compositions of these mixtures vary at high temperatures with respect to the deposited mixtures. Nevertheless, the spectra at higher temperatures were recorded, when possible, to obtain information about the band shapes and positions of the more ordered structures, but no apparent band strengths were calculated in those cases.

Together, theoretical calculations were performed for selected mixtures and structures. This allowed us to achieve a graphical picture of the vibrational modes responsible for the observed bands in the far-IR region. In most cases, we focused

on the calculations of the amorphous ices, since it was difficult to assume a certain ordered structure for the annealed ice mixtures needed to perform the calculations. In any case, comparison between the observed and calculated spectra should be regarded with caution, since theoretical spectra were not able to completely reproduce the observed spectra.

Results are shown in Sects. 3.1 and 3.2 for different ice mixtures with methanol and ammonia, respectively.

3.1. H_2O:CH_3OH ice mixtures

We studied three different compositions for the H_2O:CH_3OH ice mixture, one with a 1:1 ratio (Sect. 3.1.1), and the other two with 3:1 and 10:1 ratios, which is closer to the astrophysical scenario (Sects. 3.1.2 and 3.1.3, respectively).

Spectra were collected at 8 K for the three ice mixtures. Characterization of the annealed ice samples was performed at 130 K for the 1:1 and 3:1 ice mixtures, and at 135 K for the 10:1 ice mixture before the formation of clathrate structures (previously studied in Moore & Hudson 1994) was initiated. No desorption of water or methanol molecules was detected by the QMS at those temperatures, as expected according to the desorption temperatures reported, for example, in Martín-Doménech et al. (2014). Therefore, the column densities measured for the ices at 8 K remained constant for the annealed samples.

Table A.1 summarizes the peak frequencies and apparent band strengths of the observed far-IR features in the three mixtures, and compares them to the corresponding values for similar vibrational modes in the pure ices. The spectra from which these values are extracted are further studied in Sects. 3.1.1–3.1.3.

3.1.1. H_2O:CH_3OH 1:1

Figure 1 shows the far-IR spectrum of the H_2O:CH_3OH 1:1 ice mixture, which was deposited at 8 K and warmed up to 130 K. The ice was composed of 1.5×10^{19} molecules cm^{-2} of water, and 8.8×10^{18} molecules cm^{-2} of methanol. Column densities were calculated as explained in Sect. 2. Since the uncertainties in the column densities of these species could be of 20%−30%, or even higher, as explained in Sect. 2, we considered the ratio of this mixture to be, approximately, 1:1. Table A.1 summarizes the peak frequencies and calculated apparent band strengths of the ∼200 cm^{-1} feature observed at 8 K and the two far-IR bands (one band with a second peak at lower frequencies) detected at 130 K in Fig. 1. Band strengths were calculated assuming the above column densities.

The calculated spectrum of the amorphous ice mixture is also shown in Fig. 1. A broad band is predicted in the same region as that observed in the ice mixture, peaking at a slightly higher frequency. This broad band is due to two librational modes of water with contributions from a translational mode of water and a librational mode of methanol. A second translational mode of water with a librational mode of methanol appears as a second peak at a lower frequency with no experimental counterpart.

Figure 2 compares the far-IR spectrum of the ice mixture at 8 K with the spectra of pure water and methanol ices at the same temperature, along with the sum of the two pure ice spectra. The peak frequency of the band detected at 203 cm^{-1} in the ice mixture is slightly lower than that of the pure water ice band. A similar behavior is found for the water-dominated far-IR band in most of the mixtures studied in Moore & Hudson (1994).

A shoulder on the blue side of the water-dominated band indicates contribution of the broad band of amorphous methanol peaking at 303 cm^{-1} in the pure ice case, which is not intense enough to be clearly detected in the mixture. This was also observed in Moore & Hudson (1994). A comparison between the observed spectrum and the sum of the two pure ice spectra (scaled to the column densities of the species in the ice mixture) shows that the band strength of the water-dominated band in the mixture is similar, within errors, to the band strength of the pure water band, as shown in Table A.1. This may be because methanol and water molecules behave similarly, forming hydrogen bonds of comparable strength, and therefore, the presence of methanol molecules does not critically affect the corresponding lattice vibrational mode of water molecules.

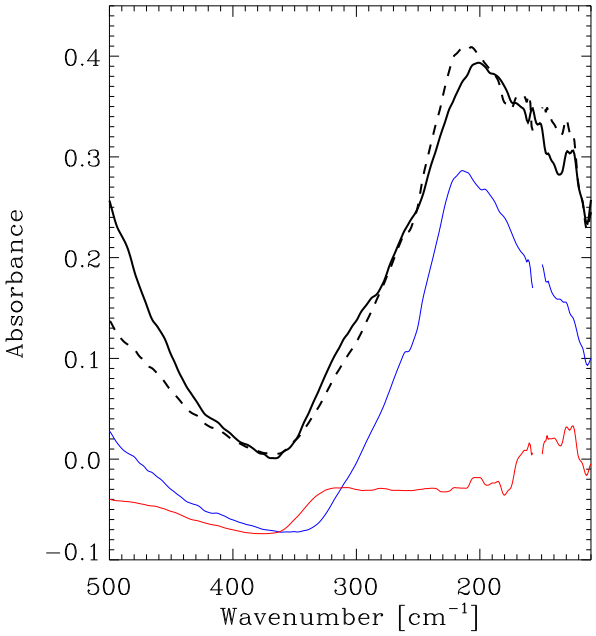

Fig. 2. Infrared spectra of an H_2O:CH_3OH 1:1 ice mixture in the far-IR region at 8 K (black solid line) along with the spectra of pure water (blue solid line) and methanol (red solid line) ices of the same thicknesses as that of each species in the ice mixture. Pure ice spectra are shifted for clarity. The dashed line is the sum of the two pure ice spectra. A small region around 150 cm^{-1} is not shown because of the high noise collected at those frequencies.

Figure 3 compares the spectrum of the annealed ice mixture at 130 K with the spectra of pure crystalline water at 150 K and pure crystalline methanol at 120 K, scaled to their column densities, as well as the sum of the two pure ice spectra. The phase change to a more ordered structure is evidenced by the appearance of a new feature in the spectrum of the ice mixture at 344 cm^{-1} (near that of pure crystalline methanol ice), and the change in the band shape of the water-dominated band, which now peaks at 215 cm^{-1}. A new peak at 170 cm^{-1} is observed in the red side of the water band, which is probably formed by contribution of both the peak of pure crystalline water at 160 cm^{-1} and the band of pure crystalline methanol at 177 cm^{-1}.

The new features in the IR spectrum of the ice mixture indicate that segregation is taking place to some extent. A comparison between the observed spectrum and the sum of the two pure ice spectra shows a decrease in the band strengths of the two main far-IR features in the ice mixture with respect to the pure ices (see Table A.1). This may indicate that segregation is not complete in the mixture, and at the same time, that the presence of other molecules affects the lattice vibrational modes in ordered structures more than in the amorphous structures, thereby slightly decreasing their band strengths.

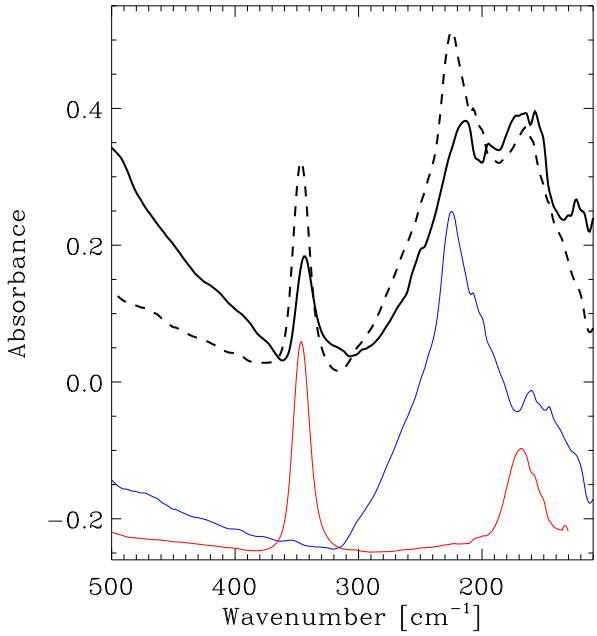

Fig. 3. Infrared spectra of an H_2O:CH_3OH 1:1 ice mixture in the far-IR region at 130 K (black solid line) along with the spectra of pure water (blue solid line) and methanol (red solid line) ices of the same thicknesses as that of each species in the ice mixture. Pure ice spectra are shifted for clarity. The dashed line is the sum of the two pure ice spectra.

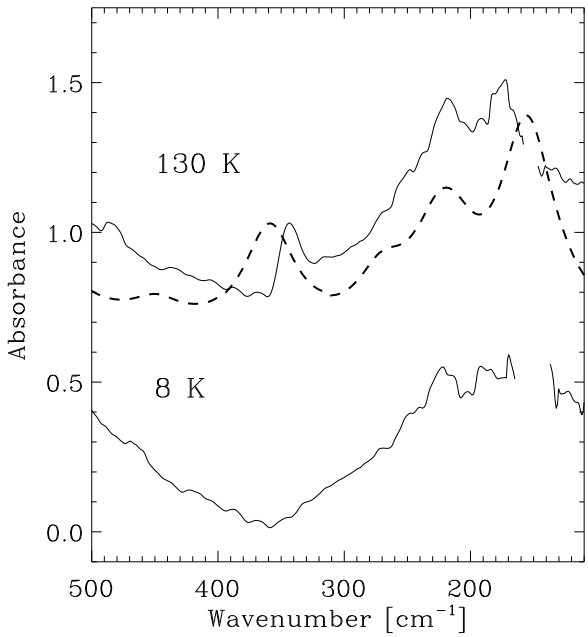

Fig. 4. Infrared spectra of an H_2O:CH_3OH 3:1 ice mixture in the far-IR region at 8 K and annealed at 130 K (solid lines). Spectra are offset for clarity. Spectral regions with high noise are not shown. The dashed line represents the calculated spectrum of an ice mixture of the same composition, which is in better agreement with the spectrum of the annealed ice.

3.1.2. H_2O:CH_3OH 3:1

Figure 4 shows the far-IR spectrum of the H_2O:CH_3OH 3:1 ice mixture, deposited at 8 K and warmed up to 130 K. The ice was composed of 2.1×10^{19} molecules cm^{-2} of water, and 7.5×10^{18} molecules cm^{-2} of methanol. The peak frequency of the water-dominated band at 8 K could not be properly measured because of the noise in that region of the spectrum. We also observe a small shoulder on the blue side of the band due to contribution of the broad band of amorphous methanol, although it is not as clear as in Figs. 1 and 2. Evolution of the spectrum during the warm up shows the same behavior as that of the 1:1 ice mixture with the three features peaking at similar frequencies within errors (see Table A.1).

The calculated spectrum of the 3:1 ice mixture shown in Fig. 4 is in better agreement with the observed spectrum of the annealed ice, since the methanol molecule included in the theoretical simulations acted as if it were segregated among the rest of water molecules. Two librational modes of water leading to one broad band in the calculated spectrum are predicted at similar frequencies as the observed peak at 215 cm^{-1}, with the contribution of two water translational modes, one of which has a less intense methanol libration. According to the calculated spectrum, the peak at 176 cm^{-1} is due to a combination of two vibrational modes, including water translation and methanol libration, which is predicted at a slightly lower frequency than in the observed spectrum.

The peak at 345 cm^{-1} resembles that of the pure crystalline methanol ice, as seen in Fig. 3. However, theoretical calculations predict a band at a slightly higher frequency due to a librational mode of water molecules. As explained in Sect. 2, these assignments should be handled with caution.

The band strength of the water-dominated far-IR band at 8 K is similar to those measured for the 1:1 mixture and the pure water ice. The presence of methanol molecules, which is less important in this mixture, does not seem to affect, in this case either, the corresponding lattice vibrational mode of the water molecules. The band strengths of the water and methanol features observed at 130 K, however, tend to be higher than in the 1:1 mixture and closer to that of the pure crystalline ices. One possible explanation for this behavior could be the longer time that the ice mixture was held at high temperatures in this experiment, which could lead to a further segregation of the molecules, and therefore, to IR features more similar to those of the pure crystalline ices.

3.1.3. H_2O:CH_3OH 10:1

Figure 5 shows the far-IR spectrum of the more astrophysical H_2O:CH_3OH 10:1 ice mixture, deposited at 8 K and warmed up to 135 K. The ice was composed of 2.0×10^{19} molecules cm^{-2} of water and 2.4×10^{18} molecules cm^{-2} of methanol. Both the spectra at 8 K and 135 K present only the water-dominated band. This is probably due to the low column density of methanol in this experiment, leading to the weakest methanol features in this series of experiments, and ultimately, to its nondetection.

3.2. H_2O:NH_3 ice mixtures

We performed three different experiments varying the ice mixtures composition. The relative amounts of the two components were chosen to investigate the behavior of, respectively, a mixture in equal amounts (H_2O:NH_3 1:1) in excess of water (H_2O:NH_3 3:1) and in excess of ammonia (H_2O:NH_3 1:3).

As in Sect. 3.1, we compared the spectra in the far-IR region of low temperature and annealed H_2O:NH_3 ice mixtures with the spectra of the pure ices. The amorphous ices were produced by fast deposition on the substrate cooled down to a temperature of 8 K. The more ordered forms were obtained by annealing up to

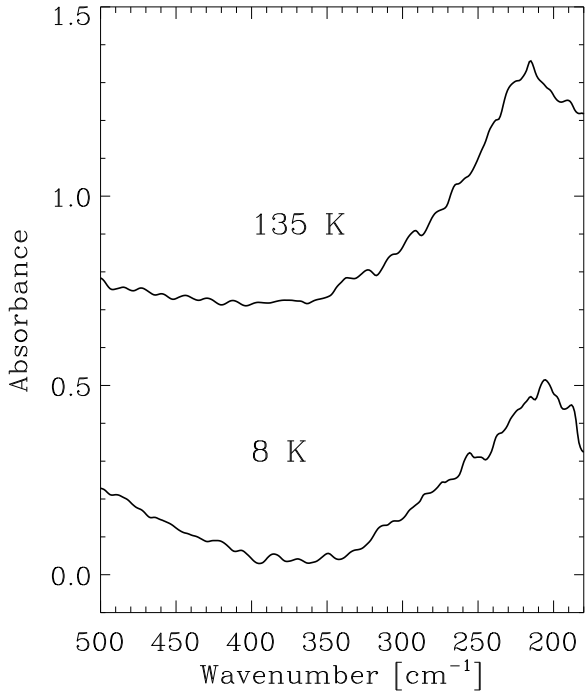

Fig. 5. Infrared spectra of an H_2O:CH_3OH 10:1 ice mixture in the far-IR region at 8 K and 135 K. Spectra are offset for clarity. The spectral window is narrower than in Figures 1 and 4 because of elevated noise in the low-frequency region of the spectrum.

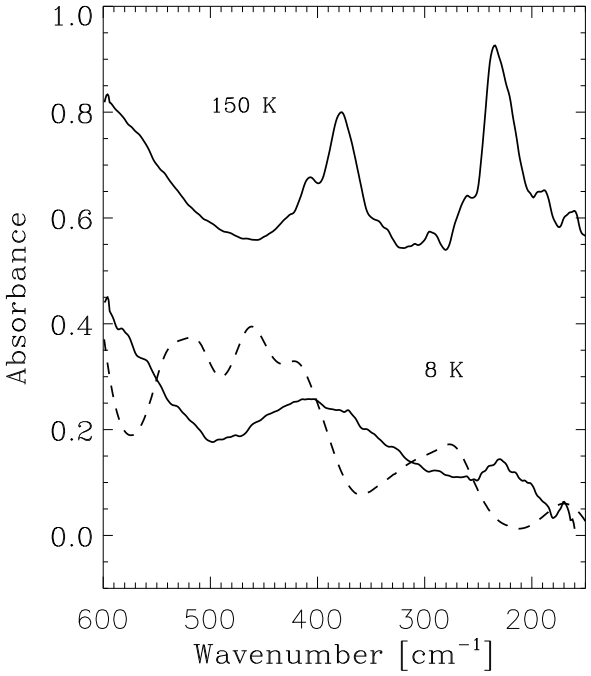

Fig. 6. Infrared spectra of an H_2O:NH_3 1:1 ice mixture in the far-IR region at 8 K and annealed to 150 K (solid lines). The H_2O:NH_3 ratio of the annealed mixture is greater than 1 because of ammonia desorption (see text). Spectra are offset for clarity. The dashed line represents the calculated spectrum of an ice mixture of the same composition.

the temperature in which the physical change could be monitored from the change in the IR spectral features.

The column densities for each mixture were calculated using the integrated optical depth of the bands at 1070, 4474, and 4993 cm^{-1} for ammonia and the band at 760 cm^{-1} for water, as mentioned in Sect. 2. The ice thickness was estimated from the calculated column density and assuming an ice density of 0.66 g cm^{-3} for ammonia (taken from Satorre et al. 2013) and 0.94 g cm^{-3} for water (from Dohnálek et al. 2003; Raut et al. 2007). The range of ice thickness investigated in these experiments varies approximately between 1 and 10 μm. The calculated column density values were only reliable for the ices at low temperature because ammonia started to desorb at temperatures higher than 90 K, as detected by the QMS. The composition of the ice mixtures were affected to an extent that was difficult to estimate, since band strengths of the mid-IR bands usually change with temperature (see, e.g., Jiménez-Escobar & Muñoz Caro 2011). Therefore, no band strengths were calculated for the more ordered structures.

In Table A.2 we present a summary of the infrared band positions and apparent band strengths (A) that are derived from the recorded spectra of the different mixtures compared with those in the pure ices. The outcome for each case is presented and discussed thoroughly in the next sections.

3.2.1. H_2O:NH_3 1:1

The recorded spectra of the H_2O:NH_3 1:1 ice mixture, which was deposited at 8 K and warmed up to 150 K, are shown in Fig. 6. The column densities for this ice were estimated to be around 7×10^{18} molecules cm^{-2} for ammonia and 1×10^{19} molecules cm^{-2} for water. The error associated with these values is on the order of 30%. The peak frequencies and calculated apparent band strengths are reported in Table A.2. A visual comparison to the simulated spectrum is also presented in Fig. 6.

The most intense features in the calculated spectrum are shifted by 50–100 cm^{-1} to higher frequencies with respect to the recorded frequency. In this calculation the vibrational modes of the ice mixture display a contribution from both components. The band predicted at 271 cm^{-1} is assigned to a librational mode of ammonia and water in various proportions. The multicomponent band at ~400 cm^{-1} is mainly assigned to a librational mode of ammonia, even if the lowest components at 420 and 459 cm^{-1} exhibit a minor contribution from water.

The position and shape of the far-IR bands of the two components in the ice mixture are affected compared with the corresponding values in the pure ice. Graphically, this behavior is shown in Figs. 7 and 8 for the disordered and more ordered phase at 8 K and 150 K, respectively.

The recorded spectrum at 8 K, shown in Figure 7, is compared to the sum of the two spectra of the pure water and ammonia ices scaled to their column densities. It is easily observed that the intensity of the band at 212 cm^{-1}, which is a water feature, is reduced compared with the same feature of the pure ice. Furthermore, the broad band at 418 cm^{-1}, indicative of the presence of ammonia, is affected to a lesser extent by the presence of water. This behavior is different to the one observed for the 1:1 H_2O:CH_3OH ice mixture at 8 K in Sect. 3.1.1. In the present case, the band strength of the water feature shows a decrease of about one order of magnitude compared to the pure ice, while in the mixture with methanol, the decrease of the water-dominated band strength is negligible. While hydrogen bonds formed between water and methanol molecules are of comparable strength to those formed between water molecules, hydrogen bonds formed between water and ammonia molecules are stronger Hagen et al. (1981). The presence of ammonia molecules in the ice thus affects the lattice vibrational mode

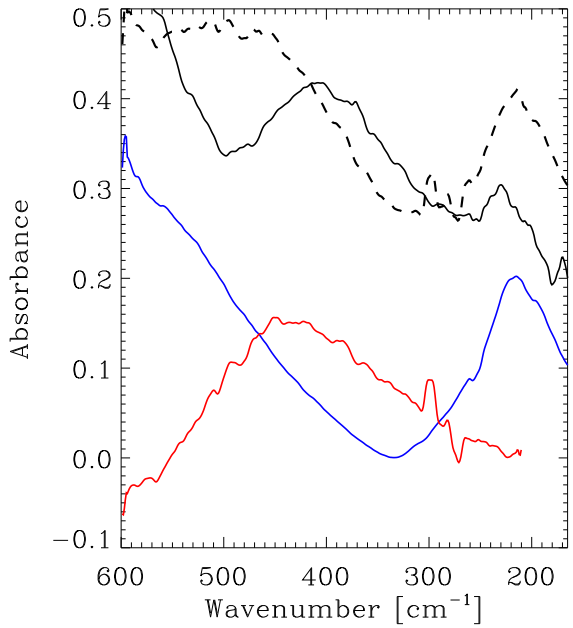

Fig. 7. Infrared spectra of an H_2O:NH_3 1:1 ice mixture in the far-IR region at 8 K (black solid line) along with the spectra of pure water (blue solid line) and ammonia (red solid line) ices of the same thicknesses as that of each species in the ice mixture. Pure ice spectra are shifted for clarity. The dashed line is the sum of the two pure ice spectra.

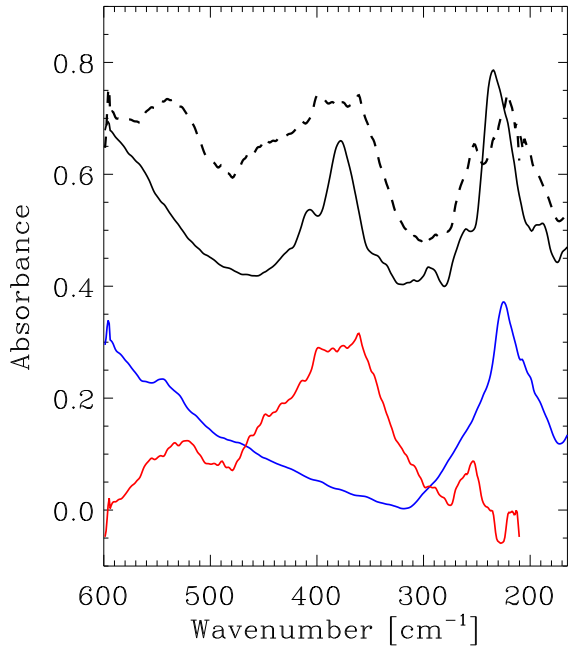

Fig. 8. Infrared spectra of an H_2O:NH_3 ice mixture deposited with a 1:1 ratio in the far-IR region at 150 K (black solid line) along with the spectra of pure water (blue solid line) and ammonia (red solid line) ices of the same thicknesses as that of each species in the deposited ice mixture. Pure ice spectra are shifted for clarity. The dashed line is the sum of the two pure ice spectra.

of the water molecules to a greater extent than the methanol molecules, decreasing the corresponding band strength.

The spectrum of the annealed ice mixture is shown in Fig. 8. As for the amorphous phase, the spectroscopic features of the mixture are compared to those of the pure crystalline ices, annealed at 70 K and 150 K for ammonia and water, respectively.

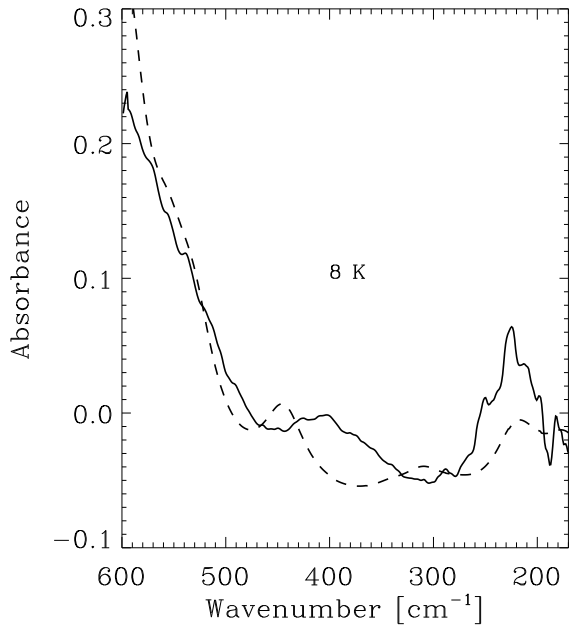

Fig. 9. Infrared spectra of an H_2O:NH_3 3:1 ice mixture in the far-IR region at 8 K (solid line). The dashed line represents the calculated spectrum of an ice mixture of the same composition.

The spectrum is also compared with the sum of the pure ice spectra. In this case, as well, the intensity of the water band in the mixture is reduced with respect to that in the pure ice.

We refer to Table A.2 for the calculated values of the far-IR apparent band strengths for ammonia and water in the 1:1 ice mixture.

3.2.2. H_2O:NH_3 3:1

Figure 9 shows the recorded spectrum for the H_2O:NH_3 3:1 ice mixture deposited at 8 K. This ice has a column density of 4×10^{18} molecules cm^{-2} for ammonia and 1×10^{19} molecules cm^{-2} for water, respectively. Unfortunately, it was not possible to record the spectrum of the annealed phase because the ice was completely evaporated before the phase transition temperature was attained.

The simulated spectrum from theoretical calculations is shown for comparison. The band predicted at 224 cm^{-1} has a strong contribution from a translational mode of water and a weaker contribution from an ammonia librational mode. The calculated band at 444 cm^{-1} is assigned to a librational mode from both ammonia and water. Although both species contribute to both vibrational modes, the contributions are not equivalent; there is a larger participation of the water motion in the lower frequency mode and of ammonia in the second, which is in agreement with the assignment proposed for the spectra of the pure ices (Giuliano et al. 2014).

The simulated spectrum does not correctly represent the relative intensities between water and ammonia far-IR bands. The water feature at 220 cm^{-1} is predicted to be less intense than the experimental feature. From the analysis of the relative intensities of the two-component features, which are shown in Fig. 10, we can observe that the mixing of the components in the ice is affecting the band strengths of the two components in a more considerable way for the less abundant component, which is ammonia in this case.

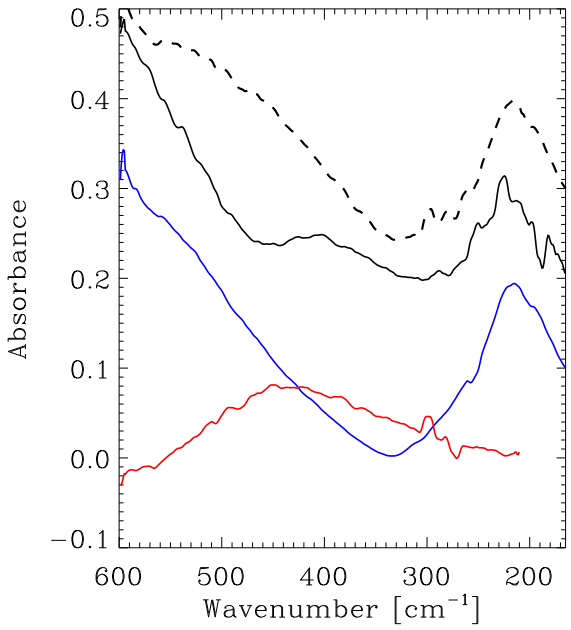

Fig. 10. Infrared spectra of an H_2O:NH_3 3:1 ice mixture in the far-IR region at 8 K (solid line) along with the spectra of pure water (blue solid line) and ammonia (red solid line) ices of the same thicknesses as that of each species in the ice mixture. Pure ice spectra are shifted for clarity. The dashed line represents the sum of the two pure ice spectra.

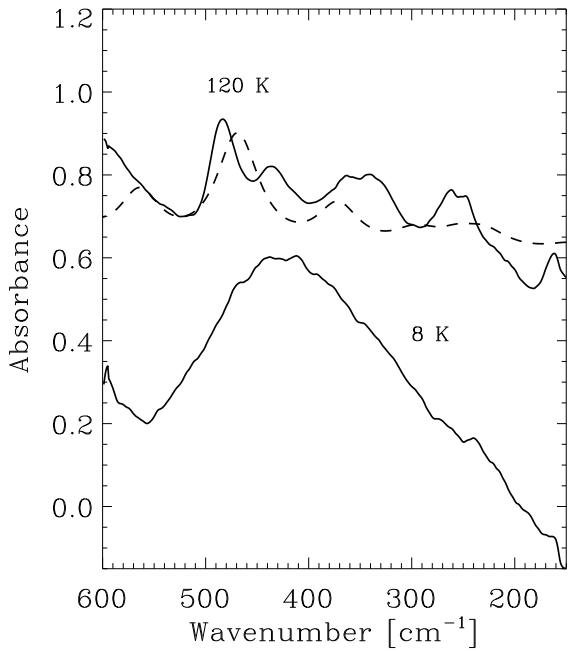

Fig. 11. Infrared spectra of an H_2O:NH_3 1:3 ice mixture in the far-IR region at 8 K and annealed at 120 K (solid lines). The H_2O:NH_3 ratio of the annealed mixture is greater than 1 due to ammonia desorption (see text). Spectra are offset for clarity. The dashed line represents the calculated spectrum of an ice mixture of the same composition, which is in better agreement with the spectrum of the annealed ice.

3.2.3. H_2O:NH_3 1:3

In order to investigate the effect on the band strengths of the two components of the mixture in excess of ammonia, we analyzed the H_2O:NH_3 1:3 ice mixture deposited at 8 K and annealed up to 120 K. This mixture has a composition of 2.4×10^{19} molecules cm^{-2} for ammonia and 8×10^{18} molecules cm^{-2} for water.

Figure 11 illustrates the spectra of the amorphous and ordered phases together with the calculated spectrum for this mixture, which shows a better agreement with the spectrum of the annealed form. The predicted bands at 372, 465, and 471 cm^{-1} are mainly assigned to ammonia librational modes with a minor contribution of water libration for the higher frequency components.

As expected from the analysis of the previous experiments, the water feature at ca 220 cm^{-1} is not visible. This effect is due to a combination of two factors. First, the dilution of the water molecules in the ice mixture contributes to a reduction of the intensity of the band; secondly, the band strength of the water feature, which is the less abundant component in the mixture, is expected to be reduced by the presence of a second component in the ice.

4. Astrophysical implications

Laboratory characterization of ice mixtures in the far-IR region provides a benchmark for ice observations in the ISM. So far, water ice is the only species detected in interstellar ices by means of far-IR spectroscopy. Omont et al. (1990), Dartois et al. (1998), and Cohen et al. (1999) observed the 44 μm feature, corresponding to water ice, from ISO data. Future planned missions like SPICA, or Herschel/PACS archive data beyond 50 μm are expected to expand the detection of ices to this wavelength range. Other ice components already detected in the mid-IR have not yet been observed in far-IR spectra. The presence of several components in the ice mantles could affect both the shape and band strengths of the far-IR features compared to the pure ice spectra, as seen in Sect. 3.1, and especially in Sect. 3.2, where band strengths are clearly decreased in the ice mixtures, compared to the corresponding values in pure ices. Minor components are the most affected species and, ultimately, overabundance of water in interstellar ices may hinder the far-IR detection of other species, as seen in Sect. 3.1.3.

Laboratory far-IR spectra of mixed ices like those studied in this work are nonetheless a more accurate benchmark to search for features corresponding to minor components. In particular, most of the NH_3 present in interstellar ices is expected to be well mixed with H_2O in the polar phase formed early during cloud evolution. This phase could also harbor a fraction of the solid CH_3OH, although most of the methanol molecules are probably contained in the CO-rich phase subsequently formed (see, e.g., Boogert et al. 2015)

Bands in the far-IR region are also significantly affected by the thermal history of the ice, since structural changes are induced when ice mantles are annealed from low to high temperatures, leading to modifications in the lattice vibrational modes. By analyzing the spectra recorded by the missions mentioned above, and comparing them to the laboratory spectra of both pure and mixed ices, information on the ice composition and structure could be derived. The column densities of the molecules in the ice could subsequently be calculated from the band strengths presented in Tables A.1 and A.2, provided that their IR features are not hindered by those of water. Even if this condition is not fulfilled, changes on the water band shape compared to the pure ice case could provide at least qualitative information on the ice composition and structure.

5. Conclusions

We have analyzed the IR spectra of astrophysically relevant ice samples in the whole spectral range from the near-IR to the far-IR spectral regions. Binary ice mixtures with different compositions of water and methanol or ammonia were studied, both in their amorphous phases at low temperature (8 K) and in more ordered structures achieved by thermal annealing to higher temperatures.

Far-IR features in the ice mixtures were usually assigned to a band in the pure ice spectra of one of the components. In the case of the annealed ice samples, the assignment was done to bands of the crystalline pure ices, indicating that segregation may be taking place to some extent.

The analysis of the spectra was supported by theoretical calculations using software programs of the Material Studio package from Dassault Systèmes Biovia Corp. A comparison between the predicted and the measured spectra allowed us to assign far-IR bands to particular vibrational modes. In general, every far-IR band was due to the contribution of vibrational modes of the two components present in the ice mixture. Bands were assigned to a particular component in the mixture when they presented a stronger contribution from the vibrational modes of that component.

Features in the near- and mid-IR regions of the spectra were used to derive column densities of the components in the ice samples. The gas phase was monitored by means of a QMS during annealing of the samples, and no ice losses were detected for water and methanol at the temperatures at which the IR spectra were collected. Ammonia was found to desorb at temperatures higher than 90 K, making the derivation of the column densities and compositions in the ice mixtures at 8 K not reliable at higher temperatures. Band strengths of the far-IR features were subsequently calculated (except for the annealed H_2O:NH_3 mixtures) and compared to the band strengths of the corresponding bands in the pure ice spectra. Band strengths in the mixtures were up to one order of magnitude lower than in the pure ices for the more critical cases. In general, larger differences were observed in those mixtures where the components were more diluted, and the nature of the components was different. In the case of water ice, band strengths in mixtures with ammonia were systematically lower than in mixtures with methanol. This could be because methanol and water molecules behave similarly, forming hydrogen bonds with a similar strength. Therefore, the presence of methanol molecules in a water ice could affect the water far-IR features to a lesser extent than the presence of ammonia molecules. In any case, these differences are higher than in the mid-IR region, since vibrational modes in the far-IR are expected to be more affected by the environment of the molecules. This is clearly supported by the theoretical calculations, where most of the modes present contribution of both components of the ice mixture, as mentioned above.

These results provide a benchmark for the analysis of observations from future space telescope missions operating in the far-IR.

Acknowledgements. B.M.G. acknowledges support from CONSOLIDER grant CSD2009-00038, led by J. Cernicharo, and M. Castellanos for his assitance. R.M.D. benefited from a FPI grant from the Spanish MINECO. This research was financed by the Spanish MINECO under Projects AYA2011-29375, AYA2014-60585-P, AYA2015-71975-REDT, CONSOLIDER grant CSD2009-00038, and FIS2013-48087-C2-1-P.

References

Anderson, A., Andrews, B., Meiering, E. M., & Torrie, B. H. 1988, J. Raman Spectrosc., 19, 85
Bertie, J. E., & Whalley, E. 1967, J. Chem. Phys., 46, 1271
Boogert, A. C. A., Gerakines, P. A., & Whittet, D. C. B. 2015, ARA&A, 53, 541
Bossa, J.-B., Maté, B., Fransen, C., et al. 2015, ApJ, 814, 47
Bouwman, J., Ludwig, W., Awad, Z., et al. 2007, A&A, 476, 995
Brown, K. G., & King, W. T. 1970, J. Chem. Phys., 52, 4437
Clark, S. J., Segall, M. D., Pickard, C. J., et al. 2005, Z. Kristallographie, 220, 567
Cohen, M., Barlow, M. J., Sylvester, R. J., et al. 1999, ApJ, 513, L135
Coustenis, A., Schmitt, B., Khanna, R. K., & Trotta, F. 1999, Planet. Space Sci., 47, 1305
Dartois, E., Cox, P., Roelfsema, P. R., et al. 1998, A&A, 338, L21
d'Hendecourt, L. B., & Allamandola, L. J. 1986, A&AS, 64, 453
Dohnálek, Z., Kimmel, G. A., Ayotte, P., Smith, R. S., & Kay, B. D. 2003, J. Chem. Phys., 118, 364
Ferraro, J. R., Sill, G., & Fink, U. 1980, Appl. Spectrosc., 34, 525
Gerakines, P. A., & Hudson, R. L. 2015, ApJ, 805, L20
Gerakines, P. A., Schutte, W. A., Greenberg, J. M., & van Dischoeck, E. F. 1995, A&A, 296, 810
Giuliano, B. M., Escribano, R. M., Martín-Doménech, R., Dartois, E., & Muñoz Caro, G. M. 2014, A&A, 565, A108
Léger, A., Klein, J., de Cheveigne, S., et al. 1979, A&A, 79, 256
Hagen, W., Tielens, A. G. G. M., & Greenberg, J. M. 1981, Chem. Phys., 56, 367
Hudgins, D. M., Sandford, S. A., Allamandola, L. J., & Tielens, A. G. G. M. 1993, ApJS, 86, 713
Jiménez-Escobar, A., & Muñoz, Caro 2011, A&A, 536, A91
Johnson, B. R., & Atreya, S. K. 1996, Icarus, 119, 405
Maeda, S., & Schatz, P. N. 1961, J. Chem. Phys., 35, 1617
Maldoni, M. M., Robinson, G., Smith, R. G., Duley, W. W., & Scott, A. 1999, MNRAS, 309, 325
Martín-Doménech, R., Muñoz Caro, G. M., Bueno, J., & Goesmann, F. 2014, A&A, 564, A8
Martonchik, J. V., Orton, G. S., & Appleby, J. F. 1984, Appl. Opt., 23, 541
Moore, M. H., & Hudson, R. L. 1992, ApJ, 401, 353
Moore, M. H., & Hudson, R. L. 1994, A&AS, 103, 45
Moore, M. H., Hudson, R. L., & Gerakines, P. A. 2001, Spectrochim. Acta A, 57, 843
Muñoz Caro, G. M., Jiménez-Escobar, A., Martín-Gago, J. Á., et al. 2010, A&A, 522, A108
Öberg, K. I., Fraser, H. J., Boogert, A. C. A., et al. 2007, A&A, 462, 1187
Omont, A., Forveille, T., Moseley, S. H., et al. 1990, ApJ, 355, L27
Perdew, J. P., Burke, K., & Ernzerhof, M. 1996, Phys. Rev. B, 77, 3865
Raut, U., Famá, M., Teolis, B. D., & Baragiola, R. A. 2007, J. Chem. Phys., 127, 204713
Sandford, S. A., & Allamandola, L. J. 1993, ApJ, 417, 815
Schmitt, B., Quirico, E., Trotta, F., & Grundy, W. M. 1998, in Solar System Ices, eds. B. Schmitt, C. de Bergh, & M. Festov (Dordrecht: Kluwer Academic Pub.), 199
Scrocco, M., Giuliani, R., & Costarelli, C. 1972, Spectrochim. Acta A, 28, 761
Sill, G., Fink, U., & Ferraro, J. R. 1980, J. Opt. Soc. Am., 70, 724
Smith, R. G., Robinson, G., Hyland, A. R., & Carpenter, G. L. 1994, MNRAS, 271, 481
Trotta, F. 1996, Thesis, LGGE – Université Joseph Fourier, Grenoble, France
Warren, S. G. 1984, Appl. Opt., 23, 1206
Warren, S. G. 1986, Appl. Opt., 25, 2650
Wexler, A. 1967, Appl. Spectroscop. Rev., 1, 29

Appendix A: Additional tables

Table A.1. Infrared band positions and apparent band strength (A) values of water-methanol mixed ices derived for the amorphous state at 8 K, and for a more ordered state at a higher temperature (n.d. stands for non detected).

Ice	Frequency (cm^{-1})	$Frequency_{pure}$ (cm^{-1})[a]	Temperature	A (cm $molec^{-1}$)[b]	A_{pure} (cm $molec^{-1}$)[c]
H_2O:CH_3OH (1:1)					
CH_3OH	n.d.	303	8	n.d.	$9.3\ (4.8) \times 10^{-20}$
H_2O	203	219		$\leq 5.5 \times 10^{-18}$[d]	$4.4\ (1.7) \times 10^{-18}$
CH_3OH	344	347	130	8.1×10^{-19}	$1.3\ (6.6) \times 10^{-18}$[e]
	170[f]	177		n.d.	$8.2\ (4.3) \times 10^{-19}$[e]
H_2O	215	227		4.6×10^{-18}[g]	$5.3\ (2.0) \times 10^{-18}$[h]
		160			
H_2O:CH_3OH (3:1)					
CH_3OH	n.d.	303	8	n.d.	$9.3\ (4.8) \times 10^{-20}$
H_2O	–[i]	219		$\leq 5.1 \times 10^{-18}$[d]	$4.4\ (1.7) \times 10^{-18}$
CH_3OH	345	347	130	1.4×10^{-18}	$1.3\ (6.6) \times 10^{-18}$[e]
	176[f]	177			$8.2\ (4.3) \times 10^{-19}$[e]
H_2O	219	227		5.5×10^{-18}[g]	$5.3\ (2.0) \times 10^{-18}$[h]
		160			
H_2O:CH_3OH (10:1)					
CH_3OH	n.d.	303	8	n.d.	$9.3\ (4.8) \times 10^{-20}$
H_2O	205	219		$\leq 8.3 \times 10^{-18}$[d]	$4.4\ (1.7) \times 10^{-18}$
CH_3OH	n.d.	347	135	n.d.	$1.3\ (6.6) \times 10^{-18}$[e]
	n.d.	177		n.d.	$8.2\ (4.3) \times 10^{-19}$[e]
H_2O	223	227		$\leq 5.5 \times 10^{-18}$[j]	$5.3\ (2.0) \times 10^{-18}$[h]
		160			

Notes. [a] Peak frequency of the related band in the pure ice, from Giuliano et al. (2014). [b] Derived in this work from the analysis of the bands in the far-IR region. [c] Band strength of the related band in the pure ice, from Giuliano et al. (2014). [d] The band corresponding to amorphous water is blended with the wide undetected band of methanol at ~303 cm^{-1}. [e] Band strength of the pure methanol ice derived at 120 K. [f] With contribution of the peak observed at ~160 cm^{-1} in the red side of the crystalline water far-IR band (see text). [g] Assuming that the band strength of the ~177 cm^{-1} vibrational mode is modified by the same factor than the ~347 cm^{-1} mode with respect to the pure ice case, and substracting the hypothetical area of the ~177 cm^{-1} band to the total area of the ~227 cm^{-1} band. [h] Band strength of the pure water ice derived at 150 K. [i] The band was detected, but the peak frequency could not be derived because of the noise in that region of the spectrum (see Fig. 4). [j] The band corresponding to crystalline water is blended with the undetected band of methanol at ~177 cm^{-1}.

Table A.2. Infrared band positions and apparent band strength (A) values of water-ammonia mixed ices derived for the amorphous state at 8 K, and for a more ordered state at a higher temperature (n.d. stands for non detected).

Ice	Frequency (cm^{-1})	$Frequency_{pure}$ (cm^{-1})[a]	Temperature (K)	A (cm $molec^{-1}$)[b]	A_{pure} (cm $molec^{-1}$)[c]
H_2O:NH_3 (1:1)					
NH_3	418	419	8	3.2×10^{-18}	8.1 (1.5) $\times 10^{-18}$
H_2O	200	219		6.8×10^{-19}	4.4 (1.7) $\times 10^{-18}$
NH_3	380	419	150	-[d]	1.2 (0.2) $\times 10^{-17}$[e]
H_2O	235	227		-[d]	5.3 (2.0) $\times 10^{-18}$
		160			
H_2O:NH_3 (3:1)					
NH_3	414	419	8	9.4×10^{-19}	8.1 (1.5) $\times 10^{-18}$
H_2O	200	219		1.8×10^{-18}	4.4 (1.7) $\times 10^{-18}$
H_2O:NH_3 (1:3)					
NH_3	440	419	8	6.9×10^{-18}	8.1 (1.5) $\times 10^{-18}$
H_2O	-[d]	219		n.d.	4.4 (1.7) $\times 10^{-18}$
NH_3	480	419	120	n.d.	1.2 (0.2) $\times 10^{-17}$[e]
H_2O	n.d.	227		n.d.	–
		160			

Notes. [a] Peak frequency of the related band in the pure ice, from Giuliano et al. (2014). [b] Derived from the analysis of the bands in the far-IR region. [c] Band strength of the pure ice, from Giuliano et al. (2014). [d] Band strengths at high temperatures were not calculated because the H_2O:NH_3 ratio changed after ammonia desorption (see text). [e] Band strength of the pure ammonia ice derived at 100 K.